

Seismic performance of precast concrete beam-column joints

J.J.Castro & H. Imai

University of Tsukuba, Ibaraki, Japan

T. Yamaguchi

Kabuki Construction Co., Ltd, Tokyo, Japan

ABSTRACT: An experimental study on seismic behavior of precast concrete beam-column joints is presented in this paper. The objective of this study is to investigate the beam-column joint seismic behavior of a newly developed precast concrete system which can make the connections more economical and easily constructed. Nine two thirds scale beam column joint specimens were tested under simulated seismic action. Test results indicated that the proposed method of connection presents an adequate strength, stiffness and ductility when subjected to large inelastic deformations under cyclic loads.

1 INTRODUCTION

During strong earthquakes, beam-column connections are subjected to severe cyclic loading. If they are not detailed properly, their performance can affect the overall response of a ductile frame structure.

Extensive researches have been conducted on precast concrete structures. However, still remain unsolved problems related with the connections of structural members which must comply with the demands of strength, ductility and energy dissipation, during the loading cycles.

In the precast concrete frame systems of the earlier days, connections between precast members were usually placed at the center of the beams and columns where smaller stresses due to earthquake forces were expected. Regardless workability problems such as transportation, made this system disadvantageous. This type of precast units is shown in Fig 1(a).

To solve this problem, another type, where the precast members are connected at the beam-column joint, was developed. This is shown in Fig 1(b). This system has many advantages, however a difficulty with the connection details is that the main bars of the precast beam need to be anchored in the joint core. Hence the column dimension need to be large enough to have the minimum anchor required by standards. Both types of precast concrete systems have the main bars embedded in the precast concrete members so that the steel and concrete connections have to be placed in the same position.

The system herein proposed, has the particularity that, the main bars are not embedded in the precast members. As shown

Fig. 1(c), the steel connections are placed in the middle part of the members where the stresses are smaller and the precast members are connected through concrete cast in situ at the beam-column joints.

In this system, when the precast members are cast corrugated metal ducts (sheath) are placed at the position of the main bars, with two lapping bars at the sides.

At the construction site, once the precast beams are positioned, the column and lower main beam bars are inserted into the sheaths, so that the bars pass straightly through the beam-column joints. Main bars are abutted at the middle of precast members, high strength mortar is then grouted inside the sheath, in such manner that the main bar stresses are transferred to the mortar and then to the lapping bars through the sheath by bond stress. Fig. 1(d) shows the outline of the connection system.

The main objective of this study was to evaluate the seismic performance of the cast

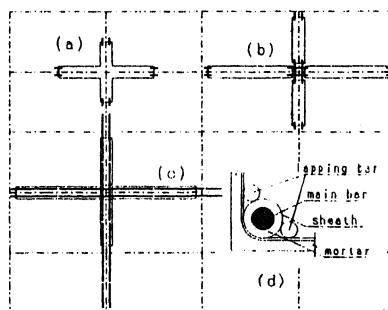


Fig. 1 Different precast concrete systems

Table 1 Characteristic of specimens

SPECIMEN		JRC-20	JPC-21	JPC-22	JPC-23	JPC-24	JPC-25	JPC-26	JPC-27	JPC-28	
C O L.	Section	50cm x 50 cm									
	Main Bars	16-D16 (SD345)				Hoops 4-D10@100 (SD345)					
	Reinf. Ratio	Pw=0.57%									
B E A M	Section	40cm x 50 cm									
	Main Bars	6-D16	4-D19	4-D22	8-D19	8-D22	6-D16	6-D16	8-D19		
	Reinf. Ratio	Pt=0.69%	0.64%	0.86%	1.35%	1.82%	0.69%	0.69%	1.35%		
	Stirrups	4D10@100 Pw=0.71%				4D13@100 1.27%		4-D10@100 0.71%			
J O I N T	Hoops	4-D10@100 Pw = 0.57%				4D13@100 0.81%		4D10@100 0.57%	2D10@100 0.28%		
	Failure Type	Beam Yielding Failure				Joint Shear Failure		Beam Yielding Failure		Joint Shear Failure	

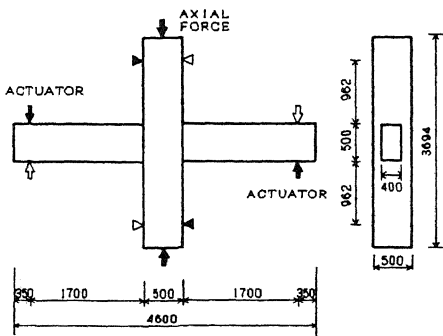


Fig. 2 Outline of the test specimen

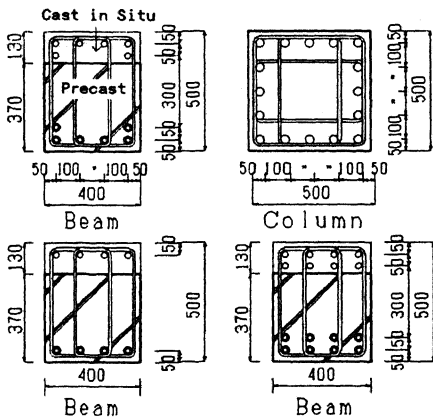


Fig. 3 Details of member sections

in situ joints which connect precast beams and columns. Others objectives were to

investigate the strength and energy dissipation of a beam-column subassemblage and to examine the behavior of the beam bars into the joint, which presents different ratios between the bar size and the column width.

2 SPECIMEN

The dimensions of a typical test specimens are showed in Fig. 2.

Nine 2/3 scale specimens were used to carry out this experiment. The specimens which represent the portion of an interior beam column subassemblage taken out from the first story of a 10 storied frame, were subjected to cyclic lateral loading with constant axial force, to simulate the earthquake action. Only the loads acting in the plane were considered.

The characteristics of the individual specimen are summarized in Table 1. The specimens were designed so that the plastic hinges in the beam ends should form prior to flexural yielding in the columns and shear failure in the beams, columns and joints, except for Specimen JPC-24, JPC-25 and JPC-28 which were designed as a joint shear failure type.

The columns had identical cross section size (50cm x 50cm) for all specimens, reinforced with 16 longitudinal bars of D16 (16 mm diameter) passing through the joint. The transverse reinforcement was welded closed rectangular hoops 4-D10 spacing every 10 cm. The beams were a composite cross section of 40cm x 50cm make up of a precast portion and the remaining section was cast later. To investigate with different ratios of column width to beam bar diameter, the longitudinal

Table 2 Material properties

SPECIMEN	JPC-20	JPC-21	JPC-22	JPC-23	JPC-24	JPC-25	JPC-26	JPC-27	JPC-28
COLUMN BARS	D16 S035 3730								
BEAM BARS	D16 3730	D19 4300	D22 4840	D19 4300	D22 4840	D16 3730	D19 4300		
STIRRUPS	D10 3620					D13 3740	D10 3620		
JOINT HOOPS	D10 3620					D13 3740	D10 3620		
Fc	BEAM	348	347	347	347	347	342	347	347
	COLUMN	348	385	385	385	344	385	375	344
	JOINT	348	319	319	319	341	319	334	341

Units: kgf/cm^2 Fc: Concrete Strength

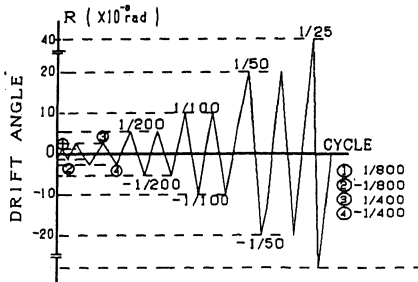


Fig. 4 Loading history

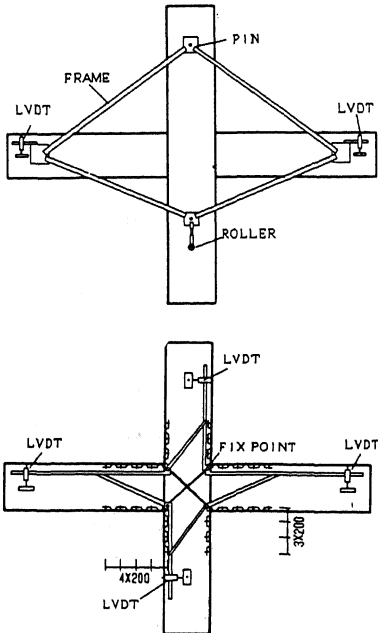


Fig. 5 Measurement devices

beam bars were placed in one or two layers depending on the specimen. All specimens had 4-D10 deformed bar stirrups spacing every 10 cm, except Specimen JPC-25 which had 4-D13.

Specimen JPC-26 was provided with two prestressing bars, to study its influence on the precast concrete. The prestressed load applied was 40 kg/cm^2 .

The specified compressive strength used for precast and cast in-situ concrete was 300 kg/cm^2 , and 600 kg/cm^2 for the grout mortar. The compressive strength of the concrete and yield strength of the reinforcing bars are shown in table 2.

All precast members were provided with shear crotters at the extreme surface of the columns and beams.

3 LOADING SYSTEM AND INSTRUMENTATION

The specimens were subjected to cyclic loads by means of vertical forces at both beam ends, so that the distribution of bending moments and shear forces will be the same as those of a beam-column joint in a laterally loaded moment resisting frame.

To simulate the gravity load 150 tons (60 Kg/cm^2) axial force was applied on the top of the column. To restrain the movement out of the plane and in the loading plane as well, both ends of the column were supported by oil jacks located at both sides. At both ends of the column, to avoid the friction, teflon plates were supplied. The loading history given is showed in Fig. 4.

There were two sets of devices to measure the deformation of specimens. The total deformation was measured with displacement transducers located at the beam ends. These transducers were fixed on a diamond shaped frame pinned at the upper column, and a roller support at the lower column. The lateral drift angle R in this paper is defined as the sum of beams displacement over the distance between the loading points.

To measure the partial deformation of members, four frames were attached to the corners of the joint. The curvature of beams, columns and joint shear distortion were measured through clip gauges as shown in Fig. 5. Strain gauges were used to monitor the strains at beams and columns reinforcement.

4 TEST RESULTS

4.1 Crack patterns

Figure 6 shows the crack patterns. For specimens designed as a beam yielding type, the cracks were concentrated mainly along the beams due to the flexural deformation, and when R was $1/100$ rad the shear cracks were observed in the joint region. In that sense JPC-20, JPC-21, JPC-27 presented very similar pattern, however JPC-23 showed similar characteristics in the beams, but the diagonal cracks in the joint presented

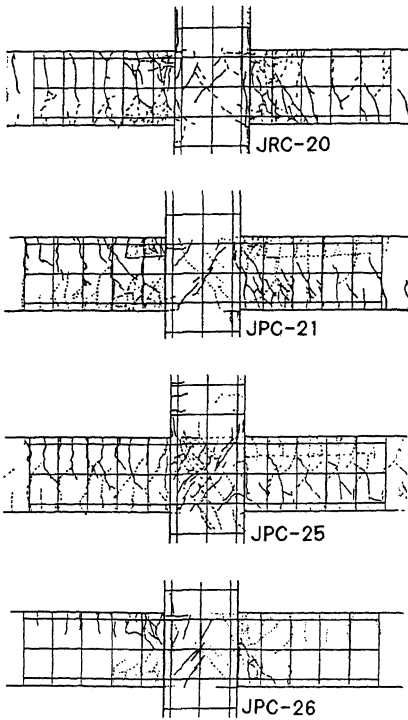


Fig. 6 Crack patterns

Table 3 Test results

Spec.	Beam Ultimate Strength				Joint Shear Stress		
	R	Q _{bu}		exp. cal.	τ _p		exp. cal.
		exp.	cal.		exp.	cal.	
JRC-20	1/30	12.8	10.8	1.18	-	-	-
JPC-21	1/30	13.2	10.8	1.18	-	-	-
JPC-22	1/30	13.7	12.4	1.1	-	-	-
JPC-23	1/30	17.1	14.7	1.16	-	-	-
JPC-24	1/30	24.2	22.8	1.06	108	100	1.08
JPC-25	1/30	27.3	27	1.01	121.8	104.2	1.16
JPC-26	1/30	13.7	10.8	1.26	-	-	-
JPC-27	1/30	13.3	10.8	1.23	-	-	-
JPC-28	1/50	24.6	22.8	1.08	109.4	94.9	1.15

exp.: observed values, cal: calculated values
 R: drift angle, F_c: concrete compressive strength
 Q_b: beam shear force, Q_{col}: column shear force
 t_p: effective width of the joint, b_c: column width
 b_s: beam width, σ_y: yielding strength of tensile reinforcement
 d_b: effective depth of the beam, t_p = (b_c+b_s)/2
 $\tau_p = \frac{Q_b L - Q_{col} h}{j_c j_b t_p}$, M_{bu} = 0.9 at σ_y d_b, Q_{bu} = M_{bu}/L
 Kamimura's Formula $\tau_p = \tau_c + \tau_s$
 $\tau_c = F_c (0.78 - 0.0016 F_c)$, $\tau_s = 0.5 P_w \sigma_y$
 Units: Q (tonf), τ (kgf/cm²)

more density. The columns did not experience any significant cracking.

JPC-24, JPC-25, JPC-28 presented a typical shear failure crack pattern, with the joint heavily affected by the shear force. The shear cracks started at R=1/400. JPC-26 showed very limited cracks along the beams

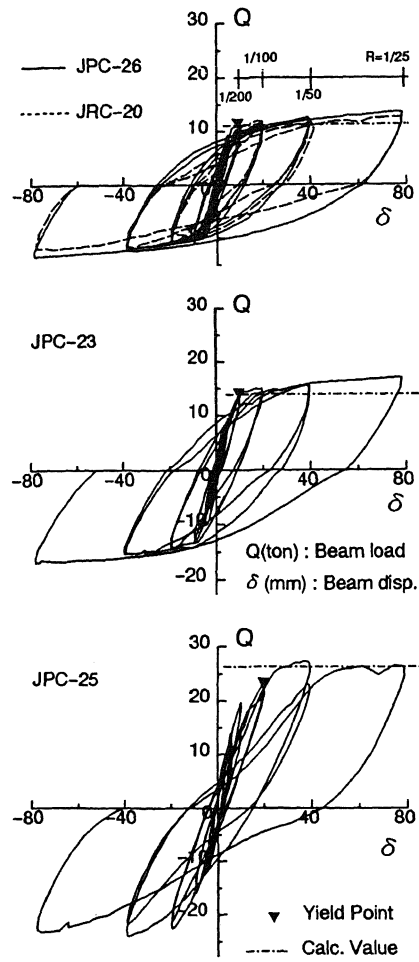


Fig. 7 Beam load-displacement relationship

and the joint as well, because of the prestressing in the beams.

4.1 Load-Deflection Relationship

The beam load vs. beam displacement relationships are shown in Fig. 7.

JRC-20, JPC-21, JPC-27 with 6 lower main bars, present very similar hysteretic shape and resistance at peak cycle deflection. The main bars started to yield at the column face once R was 1/200 rad.

JPC-22 with 4 main bars showed a similar pattern until the last cycle when a little stiffness reduction could be observed. JPC-23 also with four main bars (D 22 mm) presented good hysteretic behavior in spite of the ratio column width to bar diameter is less than 25 times. For these two specimens the main bars yielded at R=1/200, and the beams retained the maximum resistance when the displacement amplitude

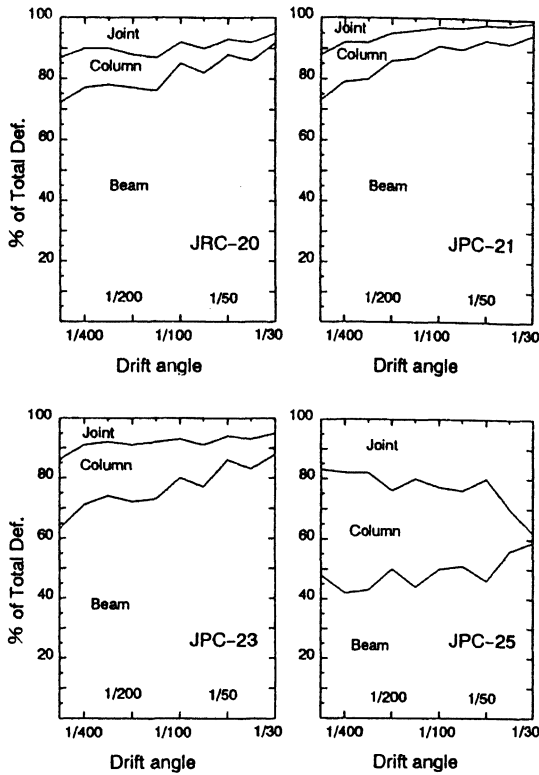


Fig. 8 Deformation components

exceeded the previous maximum value.

For JPC-24, JPC-25, JPC-28 designed as joint shear failure type, the main beam bars reached the yielding point at $R=1/100$, then the joint failed in shear. A little strength decay was observed in these three specimens at the second cycle of $R=1/50$ because of the joint shear failure.

JPC-26 showed a similar behavior than JPC-21, however since the main bars yielded at $R=1/200$ the hysteresis loop seems to have a ogival shape as a consequence of more energy dissipation.

The experimental and analytical results are shown in Table 3.

4.3 Deformation Components

Fig. 8 shows the deformation components to the total deformation at positive cycles.

There were no much differences between JRC-20 and JPC-21, however the joint deformation of JPC-21 decreased with the loading cycles. JPC-27 which had half of the joint reinforcement (ρ_w) that JRC-20 shows similar pattern but the joint component was slightly bigger. In these three cases after the beam bars yielded the beam deformation component was about 90%.

JPC-23 shows a column and joint defor-

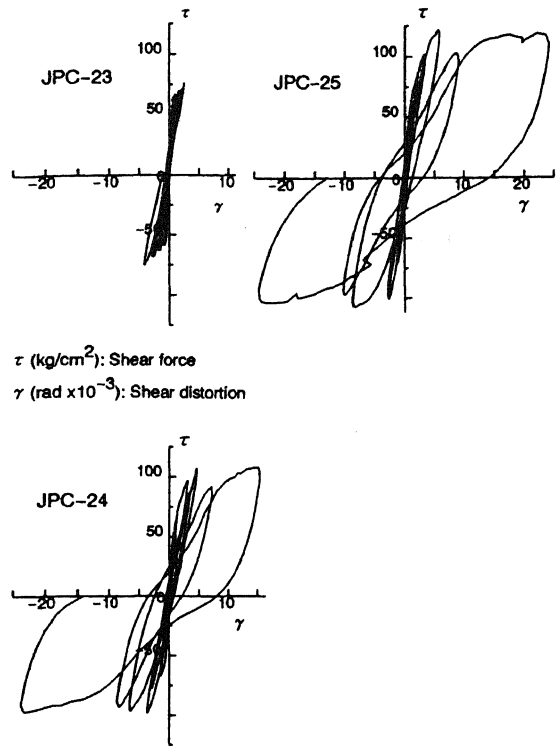


Fig. 9 Joint shear distortion

mation as well, a little bigger than JPC-22 which had also the same bar arrangement but with smaller reinforcement ratio ρ_t .

JPC-24 and JPC-28 present similar values for the deformation components up $R=1/50$ where the joint failed in shear. However after that, the joint deformation component for JPC-28 increased significantly. For JPC-25 the joint failed in shear at $R=1/50$. In this specimen the column also failed at the same loading stage.

4.4 Joint shear distortion

The joint shear stress vs. shear distortion relationship are shown in Fig. 9. The effective joint area to resist the shear stress is defined as the column effective depth multiplied by the average of the beam and column widths.

There was no significant difference among the specimens designed as beam yielding type, where the joint shear distortion was insignificant.

JPC-24 and JPC-28 present similar hysteretic curves up to $R=1/50$ rad where the joints failed in shear. Thereafter at the last cycle the joint deformation for JPC-28 was 30% bigger than that of JPC-24. At this point both specimens reached the maximum

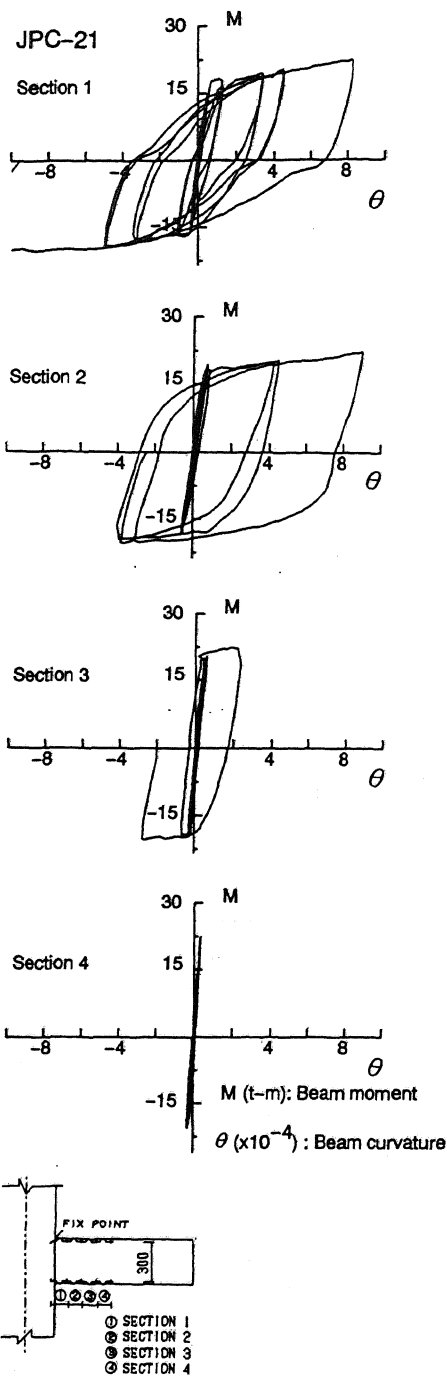


Fig. 10 Moment-curvature of beams

shear stress. Also JPC-25 failed in shear, but at 1/50 the shear stress reached the maximum value.

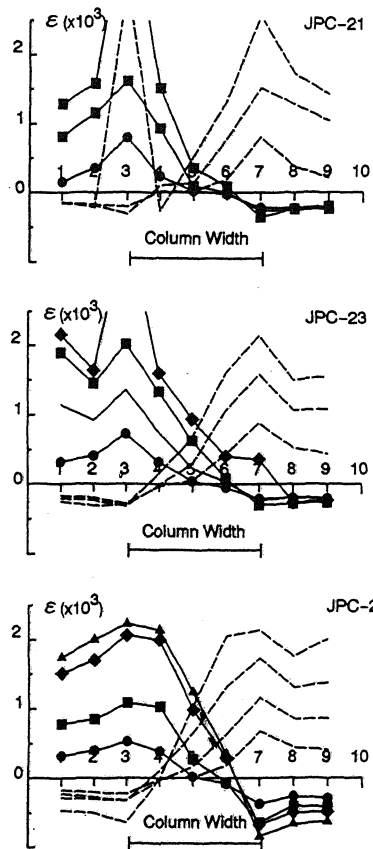


Fig. 11 Strain distribution of beam bars

4.5 Moment-curvature of beams

Figure 10 presents the moment defined at the column face vs. curvature at different sections along the beams. The sections are defined by the positions of the clip gauges attached to beams. The hysteretic curves for the section adjacent to the column face showed that the beams behaved almost in elastic way up to $R=1/200$. Then when the main bars started to yield, the hysteretic loops degraded. For the specimens designed as a beam yielding type, the curvatures observed shows that the deformation was concentrated not only in the section adjacent to the column, but also spread along the beam, at least up to the second section defined by the clip gauges.

4.6 Strain distribution

Measured strains along the length of the bottom longitudinal bars are showed in Fig. 11. Solid lines represents the distribution during the positive loading direction and the broken lines in the negative.

The compressive side of the critical sections of the beam for main bars showed no tendency to change from the assigned compression strains to tension before yielding in tension side. No differences were observed between the behavior of top bars embedded in the cast in situ concrete and the bars located in the precast members.

All specimens showed good bond behavior inside the joint.

5 CONCLUSIONS

Based on the test results the following conclusions can be drawn.

- 1) Specimens designed as beam yielding type showed a very ductile behavior. The present precast concrete connections sustained inelastic deformations and can be as ductile as those cast in-situ.
- 2) No bond deterioration was observed inside the joint up to $R=1/50$.
- 3) The deformation was concentrated not only at the critical section but also spread about 40cm from the column face along the beam.

REFERENCES

- Yanez, R.; Yamaguchi, T. & Imai, I. 1992
"Bond performance of lapping joint developed for precast concrete columns" 10WCEE
- Imai, H.; Yamaguchi, T.; Kobayashi, T.;
"Study on seismic performance of precast concrete columns with lapping joints under shear forces." 10WCEE